

## NOTES AND CORRESPONDENCE

**Climate Response to Rapid Urban Growth: Evidence of a Human-Induced Precipitation Deficit**

ROBERT K. KAUFMANN,\* KAREN C. SETO,<sup>+</sup> ANNEMARIE SCHNEIDER,<sup>#</sup> ZOUTING LIU,<sup>@</sup> LIMING ZHOU,<sup>&</sup>  
AND WEILE WANG\*\*

*\*Center for Energy and Environmental Studies, Boston University, Boston, Massachusetts*

*+Department of Geological and Environmental Sciences, Stanford University, Stanford, California*

*#Department of Geography and Institute for Computational Earth System Science, University of California, Santa Barbara, Santa Barbara, California*

*@Guangdong Meteorological Bureau, Guangzhou, China*

*&School of Earth and Atmospheric Sciences, Georgia Institute of Technology, Atlanta, Georgia*

*\*\*Foundation of California State University, Monterey Bay, California*

(Manuscript received 15 November 2005, in final form 8 September 2006)

## ABSTRACT

The authors establish the effect of urbanization on precipitation in the Pearl River Delta of China with data from an annual land use map (1988–96) derived from Landsat images and monthly climate data from 16 local meteorological stations. A statistical analysis of the relationship between climate and urban land use in concentric buffers around the stations indicates that there is a causal relationship from temporal and spatial patterns of urbanization to temporal and spatial patterns of precipitation during the dry season. Results suggest an urban precipitation deficit in which urbanization reduces local precipitation. This reduction may be caused by changes in surface hydrology that extend beyond the urban heat island effect and energy-related aerosol emissions.

**1. Introduction**

Urban land use change has been and will continue to be one of the biggest human impacts on the terrestrial environment. At the start of the 1900s, there were only 16 cities with populations over 1 million; by 2000, there were 417 (UNCHS 2002). Some of these cities were built in the Pearl River Delta, which is located in southeast China. Here, cities have grown rapidly due to changes in the policy and economic environment (Yeh and Li 1997, 1998; Weng 2002; Seto and Kaufmann 2003).

The expansion of these cities follows a particular spatial and temporal form: recent studies show that despite differences in levels of economic development and local policies, there are common patterns in the shape, size, and growth of urban land across urban zones and cities

in the Pearl River Delta region (Seto 2004; Seto and Fragkias 2005). There is also evidence that disconnected urban areas converge toward a pattern of contiguous urban fabric.

Building cities on previously vegetated surfaces modifies the exchange of heat, water, trace gases, aerosols, and momentum between the land surface and overlying atmosphere (Crutzen 2004). In addition, the composition of the atmosphere over urban areas differs from undeveloped areas (Pataki et al. 2003). These changes imply that urbanization can affect local, regional, and possibly global climate at diurnal, seasonal, and long-term scales (Zhou et al. 2004; Zhang et al. 2005).

Here we examine the effect of urban expansion on precipitation in the Pearl River Delta of China with satellite-derived measures of annual urban extent (1988–96) and monthly climate data from 16 local meteorological stations. Statistical analysis of the relationship among precipitation, temperature, and urban land use in concentric buffers around meteorological stations indicates that there is a causal relationship from

---

*Corresponding author address:* R. Kaufmann, Center for Energy and Environmental Studies, Boston University, 675 Commonwealth Avenue, Suite 141, Boston, MA 02215.  
E-mail: Kaufmann@bu.edu

temporal and spatial patterns of urban land use to temporal and spatial patterns of precipitation that may reduce rainfall during the dry season. These results constitute the first statistically meaningful empirical evidence for an “urban precipitation deficit.” This effect may be generated by changes in surface hydrology that reduce the flow of water from the land to the atmosphere. Because 60% of the world’s population may live in urban areas by 2030 (UN 2002), urbanization may exacerbate climatic alterations associated with changes in radiative forcing.

## 2. Urban growth and its impacts on local climate

Research over the last two decades has generated significant understanding of the relationship between urban areas and climate. Many of these studies have been extensively reviewed in the literature (Souch and Grimmond 2006; Kanda 2006; Shepherd 2005; Voogt and Oke 2003). Here we summarize a few key findings relevant to our study.

There is now a coherent understanding of urban surface energy balance dynamics, with a well-established urban heat island effect that appears stronger during the night than the day (Lo et al. 1997; Banta et al. 1998). This effect is thought to be generated by the interaction among building geometry, land use, and urban materials (Oke 1976; Wang et al. 1990; Arnfield 2003).

Numerous studies evaluate the relationship between urban areas and precipitation (Shepherd 2005). These studies are based on static comparisons between metropolitan regions and their rural surroundings. They have generated a general consensus that urbanization affects precipitation, but the mechanism(s) by which urbanization affects precipitation is poorly understood (Lowry 1998). Mechanisms discussed include 1) enhanced convergence due to increased surface roughness in the urban environment (Thielen et al. 2000), 2) destabilization due to urban heat island (UHI)-thermal perturbation of the boundary layer and the resulting downstream translation of the UHI circulation or UHI-generated convective clouds (Shepard et al. 2002), 3) enhanced aerosols in the urban environment for cloud condensation nuclei sources (Molders and Olson 2004), or 4) bifurcating or diverting precipitating systems by the urban canopy or related processes (Bornstein and Lin 2000). Others have hypothesized that urban areas serve as moisture sources needed for convective development (Dixon and Mote 2003).

Even less understood is the relationship between urban growth—or land conversion—and local climate. While numerous studies focus on urban climate, few examine urban growth explicitly (Tereshchenko and Filonov 2001; Deosthali 2000; Ji et al. 2006).

## 3. Data and methodology

The study area is defined by one Landsat Thematic Mapper (TM) scene (26 000 km<sup>2</sup>) of the Pearl River (*Zhujiang*) Delta, which is located in the southern Chinese province of Guangdong, between 21° and 23°N (Fig. 1). This area has a dry season during a temperate winter and a rainy season (May through September) during a long summer.

Estimates for urban growth are extracted from Landsat TM images for each of 9 yr, 1988 to 1996. The month in which the image is acquired varies by year, but all are acquired during the dry season between October and March. From these images, we generate annual maps (30 m × 30 m resolution) for urban areas (Seto et al. 2002; Kaufmann and Seto 2001). Temperature and precipitation data are obtained from 16 meteorological stations that lie within the image (Fig. 1). Monthly data for daily average temperature and total precipitation are compiled for winter (December–February), spring (March–May), summer (June–August), and autumn (September–November).

Around each station, we establish three concentric buffers that have a radius of 3, 10, and 20 km. For each of 48 buffers (3 sizes × 16 stations), we calculate the fraction of total area that is urban (Frac) for each year (1988–96). To determine whether the pattern of urbanization affects precipitation, we also calculate two spatial metrics for urbanization (McGarigal and Marks 1995). Urban edge density (ED) measures the total edge of urban areas relative to the total landscape and is calculated as follows:

$$ED = \frac{E}{A}(10000), \quad (1)$$

in which  $E$  is the total length (m) of edge in the buffer and  $A$  is the total buffer area (m<sup>2</sup>). The ratio is multiplied by 10 000 to convert square meters to hectares.

The landscape shape index (LSI) provides a standardized measure of perimeter length of all patches of a given land cover type. The landscape shape index is calculated as follows:

$$LSI = \frac{E}{\min E}, \quad (2)$$

in which  $E$  is the total length of edge in landscape in terms of number of cell surfaces and includes all landscape boundary and background edge segments, and  $\min E$  is the minimum total length of edge in landscape in terms of number of cell surfaces.

To determine whether urbanization affects precipitation, we use the notion of Granger causality (Granger

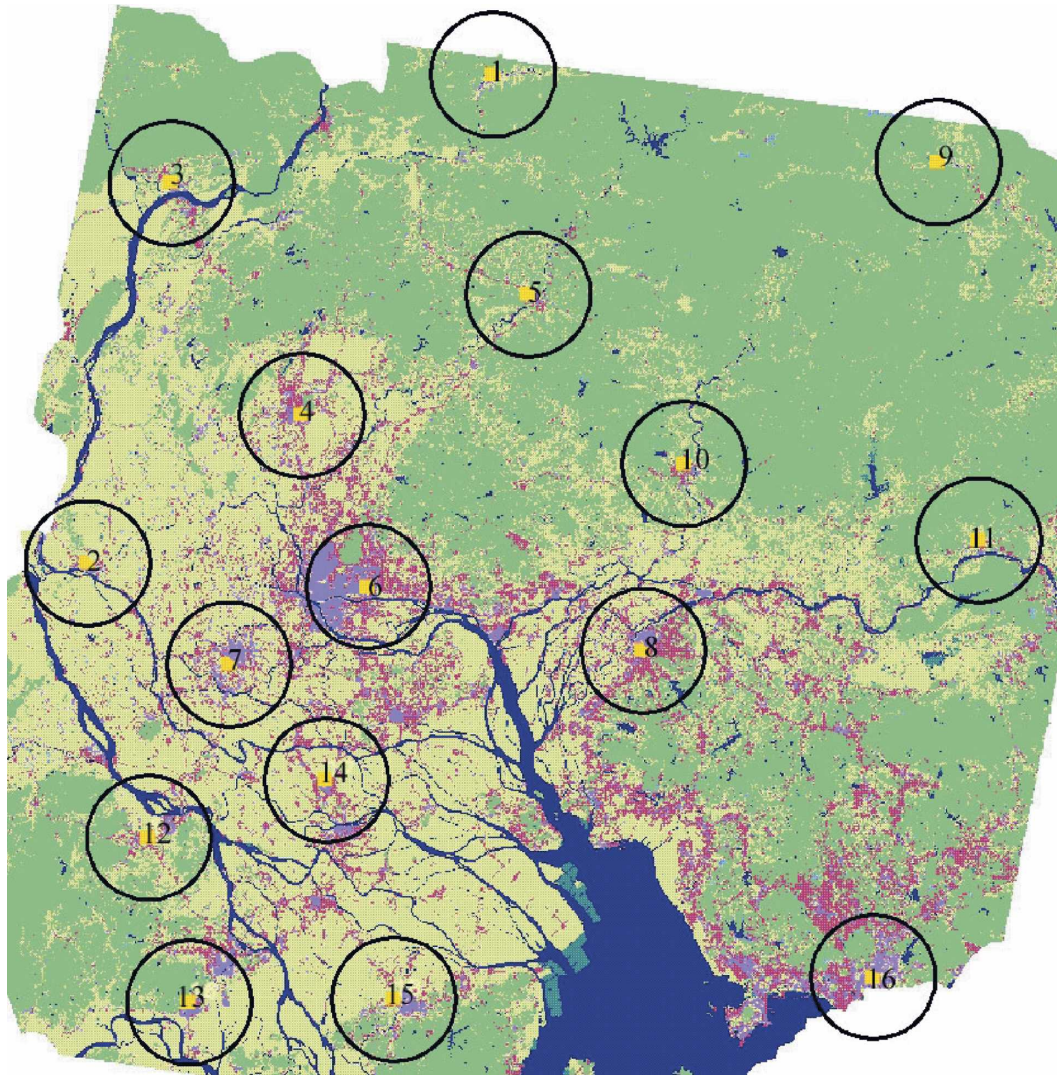


FIG. 1. The 16 meteorological stations and the 10-km buffers. Urban areas are shown in magenta. Meteorological stations (1) Fogang, (2) Sanshui, (3) Qingyuan, (4) Huadu, (5) Conghua, (6) Guangzhou, (7) Nanhai, (8) Dongguan, (9) Longmen, (10) Zengcheng, (11) Boluo, (12) Heshan, (13) Xinhui, (14) Shunde, (15) Zongshan, and (16) Shenzhen.

1969, 1980). Although Granger causality does not imply a physical causal relationship, the methodology is used to investigate physical systems, including the relationship between surface features and local climate (Kaufmann et al. 2003; Mosedale et al. 2006). A causal relationship from the urbanization variable to precipitation is estimated from Eq. (3):

$$\begin{aligned}
 P_{s,i,t} = & \alpha + \beta_1 \text{Year}_t + \beta_2 \text{Urban}_{s,i,t-1} + \beta_3 T_{s-1,i,t} \\
 & + \beta_4 P_{s-1,i,t} + \beta_5 \left( \frac{1}{N-1} \sum_{k=1, k \neq i}^N T_{s,i,t} \right) \\
 & + \beta_6 \left( \frac{1}{N-1} \sum_{k=1, k \neq i}^N P_{s,i,t} \right), \quad (3)
 \end{aligned}$$

in which  $P$  is observed precipitation during season  $s$  for station  $i$  at time  $t$ , Year is the year in which the image is acquired, Urban is either the fraction urban (Frac) or one of the spatial metrics for urbanization (e.g., ED or LSI), and  $T$  is temperature. Temperature is included to represent any cotemporaneous correlation between temperature (the urban heat island effect or other change) and precipitation. Current values of temperature and precipitation at the other 15 meteorological stations are included to represent conditions at a regional scale. If the region is warming or drying due to changes other than local urbanization, including regional averages will reduce the likelihood that the statistical methodology will mistakenly attribute them to local urbanization. From a statistical perspective, their

inclusion reduces any cross correlation of the regression errors due to large-scale events, and this will increase the efficiency of the estimation.

Equation (1) can be specified and estimated using a variety of assumptions about variations in the intercept ( $\alpha$ ) and slopes ( $\beta_i$ ) among the 16 stations. Specifically, Eq. (3) can assume that (a) the intercept and slopes are the same across all 16 stations; (b) the intercept varies across the 16 stations, but the slopes are the same; and (c) the intercept and slopes vary across stations. Each assumption requires a different estimation technique. If the intercept and slopes are the same across stations, Eq. (3) is estimated using ordinary least squares. If the intercept varies across the 16 stations, but the slopes are the same, Eq. (3) is estimated using either a fixed or random effect estimator. If the intercept and slopes vary across stations, Eq. (3) is estimated using a random coefficient model, which assumes that coefficients for individual stations vary randomly around a constant mean.

There is no a priori justification for choosing an assumption about spatial variations in the regression coefficients; therefore, we chose among specifications and estimation techniques using test statistics (Mundlak 1978; Hsiao 1986). In summary, we start with the least restrictive assumption, the slope and/or intercepts vary among stations (random coefficient model) and test whether restrictions that equalize the intercept and slopes across stations increase the residual sum of squares in a statistically meaningful fashion. If they do, the less restrictive assumption is used to estimate Eq. (3). The number of lags, one, is the maximum value that allows us to perform these tests on the nine observations per station. A value of one lag implies that the version of Eq. (3) used to estimate summer precipitation specifies springtime values for temperature and precipitation.

Granger causality from the urbanization variable to precipitation is indicated by the statistical significance of  $\beta_2$  in Eq. (3). Rejecting the null hypothesis  $\beta_2 = 0$  indicates that the lagged value of the urbanization variable has information about the current value of precipitation beyond that contained in the lagged values of precipitation, temperature, time, and average values for current temperature and precipitation in the other 15 stations. This would provide statistical evidence that the urbanization variable “Granger causes” precipitation.

We extend the analysis of Granger causality by testing whether Eq. (3) (unrestricted model) generates a more accurate out-of-sample forecast than a restricted version of Eq. (3) (restricted model), in which the

lagged value of the urbanization variable is eliminated by imposing  $\beta_2 = 0$  (Granger and Huang 1997):

$$P_{s,i,t} = \alpha + \beta_1 \text{Year}_t + \beta_3 T_{s-1,i,t} + \beta_4 P_{s-1,i,t} + \beta_5 \left( \frac{1}{N-1} \sum_{k=1, k \neq i}^N T_{s,k,t} \right) + \beta_6 \left( \frac{1}{N-1} \sum_{k=1, k \neq i}^N P_{s,k,t} \right). \quad (4)$$

The out-of-sample forecast generated from Eqs. (3) and (4) can be calculated using two methods. One method eliminates observations for a single year from the sample data, estimates Eqs. (3) and (4), and uses those equations to generate an out-of-sample forecast for the year omitted from the sample. This process is repeated for all years for which lagged values are available. The other method eliminates the nine observations from a single station from the sample, estimates Eqs. (3) and (4) from the observations for the remaining 15 stations, and uses these equations to generate an out-of-sample forecast for the nine observations for the station that is excluded from the sample. This process is repeated for each of the 16 stations.

Of these two methods, we generate the out-of-sample forecast by eliminating a single station from the sample and repeating this process 16 times so that we have an out-of-sample forecast for every year and station. This generates 144 observations. Fewer observations would be available using the alternative method because the lagged values in Eqs. (3) and (4) would prevent us from estimating those equations for the year excluded from the sample and the year that follows.

Furthermore, generating the out-of-sample forecast by eliminating observations from a single meteorological station increases the power of analysis (Granger and Huang 1997). Granger and Huang (1997) argue that generating the out-of-sample forecast by excluding individuals is a more powerful method of testing Granger causality than generating an out-of-sample forecast by excluding observations across individuals for a given period. They warn that this power is lost if the test statistic used to compare forecasts is affected by errors that covary or are heteroscedastic.

To avoid the effects of covariance and/or heteroscedasticity, we evaluate the out-of-sample forecasts generated by Eqs. (3) and (4) using two parametric tests, the sign test and the signed rank test (Lehmann 1975). To calculate these test statistics, we use the following loss function:

$$d_t = (P_{s,i,t} - \hat{P}_{s,i,t,U})^2 - (P_{s,i,t} - \hat{P}_{s,i,t,R})^2, \quad (5)$$

in which  $P_{s,i,t}$  is the observed value for precipitation during season  $s$  for station  $i$  at time  $t$ ,  $\hat{P}_{s,i,t,U}$  is the out-of-sample forecast for precipitation generated by the unrestricted model [Eq. (3)], and  $\hat{P}_{s,i,t,R}$  is the out-of-sample forecast generated by the restricted model [Eq. (4)]. Values of  $d$  are used to calculate the  $S_{2a}$  [Eq. (6)] and  $S_{3a}$  [Eq. (7)] statistics (Lehmann 1975) as follows:

$$S_{2a} = \frac{\sum_{t=1}^N I_+(d_t) - 0.5N}{\sqrt{0.25N}} \quad (6)$$

$$S_{3a} = \frac{\sum_{t=1}^N I_+(d_t)\text{rank}(|d_t|) - \frac{N(N+1)}{4}}{\sqrt{\frac{N(N+1)(2N+1)}{24}}}, \quad (7)$$

$$I_+(d_t) = 1 \quad \text{if } d_t > 0 = 0 \quad \text{otherwise}$$

in which  $N$  is the number of observations ( $9 \times 16 = 144$ ).

The  $S_{2a}$  and  $S_{3a}$  statistics test the null hypothesis that the accuracy of the out-of-sample forecasts is equal (i.e.,  $d = 0$ ). A negative value for the  $S_{2a}$  or  $S_{3a}$  statistic that exceeds the  $p = 0.05$  threshold ( $-1.96$ ) indicates that eliminating the urbanization variable from Eq. (3) reduces the accuracy of the out-of-sample forecast generated by Eq. (4). Such a result would imply that lagged values of urbanization have information about current values of precipitation that extends beyond the other variables in Eq. (3). Under these conditions, we would conclude that urbanization Granger causes precipitation (Granger and Huang 1997).

#### 4. Results and discussion

Restrictions that equalize the slopes and/or intercept among meteorological stations generally are not rejected. The slopes and intercept are the same among stations for 22 equations, and these equations are estimated using ordinary least squares (Table 1). The random effects estimator is used to estimate six equations, for which the intercept varies among stations and the slopes are the same. Finally, test statistics reject restrictions that equalize the slopes or intercept for eight equations; therefore, these equations are estimated using the random coefficient model.

The presence/absence of a causal relationship from urbanization to precipitation varies by season and buffer size (Table 1). Results reject the null hypotheses that  $\beta_2 = 0$  and that the  $S_{2a}$  and  $S_{3a}$  statistics equal zero for winter. For spring and fall, results generally reject  $\beta_2 = 0$  but fail to reject the null hypothesis that the  $S_{2a}$

TABLE 1. Regression results for Eq. (3) and tests of predictive accuracy for out-of-sample forecasts. Coefficients are statistically significantly different from zero at \*\*1%, \*5%, and +10% levels. Equation (3) is estimated using ordinary least squares (\$), random effects (#), and random coefficient model.

	Winter			Spring			Summer			Fall		
	$\beta_2$	$S_{2a}$	$S_{3a}$	$\beta_2$	$S_{2a}$	$S_{3a}$	$\beta_2$	$S_{2a}$	$S_{3a}$	$\beta_2$	$S_{2a}$	$S_{3a}$
Frac	$-4.80 \times 10^{3\$}$	-0.94	-1.40	$-1.39 \times 10^{4\#\$}$	-0.53	-0.30	$-3.84 \times 10^{3\$}$	-0.71	0.16	$-3.01 \times 10^{3\dagger}$	0.88	2.16*
ED	$-2.79 \times 10^{2\#\$}$	-2.83*	-1.81 <sup>+</sup>	$-3.83 \times 10^{1\$}$	-0.88	-0.59	$-9.13 \times 10^{1\#\$}$	-2.48*	-1.92 <sup>+</sup>	-9.89 <sup>\\$</sup>	1.23	0.96
LSI	-1.32 <sup>\\$</sup>	1.89 <sup>+</sup>	2.46*	$-6.02 \times 10^{2*\dagger}$	2.12*	2.77*	$-1.79 \times 10^{2\#\$}$	-0.18	-1.23	$1.40 \times 10^{1\$}$	0.35	0.86
Frac	$-5.93 \times 10^{3\#\$}$	-1.13	-1.46	$-3.20 \times 10^{4\#\#}$	-2.12*	-2.64*	$-3.69 \times 10^{3\$}$	-0.53	0.27	$-1.20 \times 10^{5*\#\dagger}$	0.53	1.51
ED	$-2.03 \times 10^{3\#\$}$	-1.13	-1.47	$3.36 \times 10^{2\#\#}$	2.12*	1.58	$-9.03 \times 10^{2\$}$	0.00	0.04	$-5.78 \times 10^{2*\#\dagger}$	0.35	0.79
LSI	$-2.67 \times 10^{2+\$}$	-1.70 <sup>+</sup>	-1.41	$-1.14 \times 10^{4\#\#}$	-1.24	-2.51*	$-6.45 \times 10^{3\$}$	-0.88	-0.58	$-3.93 \times 10^{4*\#\dagger}$	0.18	0.88
Frac	$-9.10 \times 10^{2+\$}$	-2.46*	-1.77 <sup>+</sup>	$-3.99 \times 10^{4\#\#}$	-1.94 <sup>+</sup>	-2.84*	$-9.63 \times 10^{3\$}$	-0.71	0.26	$-1.42 \times 10^{5*\#\dagger}$	0.71	2.08*
ED	$-2.96 \times 10^{2+\$}$	-2.65*	-1.60	$-1.19 \times 10^{4\#\#}$	-1.94 <sup>+</sup>	-2.93*	$-8.47 \times 10^{3\$}$	-0.71	-0.41	$-3.73 \times 10^{4*\#\dagger}$	1.59	2.43*
LSI	$-3.34 \times 10^{3+\$}$	-2.65*	-1.59	$-1.35 \times 10^{4\#\#}$	-1.94 <sup>+</sup>	-2.93*	$-9.61 \times 10^{3\$}$	-0.71	-0.41	$-4.20 \times 10^{4*\#\dagger}$	3.36*	4.40**

3-km buffer

10-km buffer

20-km buffer

and  $S_{3a}$  statistics are zero. For summer, results fail to reject the null hypothesis  $\beta_2 = 0$  (except for two cases) and always fail to reject the null hypothesis that the  $S_{2a}$  and  $S_{3a}$  statistics are zero. These results indicate that urbanization Granger causes precipitation during winter, with suggestions of a weaker effect during spring and fall.

For all seasons, results for the 3-km buffer are less likely to reject the null hypotheses  $\beta_2 = 0$  and/or that the  $S_{2a}$  or  $S_{3a}$  statistic equals zero. Results for the 10- and 20-km buffers reject the null hypotheses  $\beta_2 = 0$  and/or that the  $S_{2a}$  and  $S_{3a}$  statistics equal zero for winter, spring, and fall. Results do not differ between the 10- and 20-km buffers. Nor do the results differ among the measures of urbanization metrics. These results suggest that the effect of urbanization on precipitation is generated at scales of hundreds of square kilometers (the 3-km buffers are less than 30 km<sup>2</sup>, and the 10-km buffers are more than 300 km<sup>2</sup>). Furthermore, this effect is not generated solely by the pattern of urbanization; the causal relationship appears when Frac is used as the urbanization variable.

For seasons and buffer sizes that show a causal relationship between urbanization and precipitation,  $\beta_2$  generally is negative. This would seem to imply that increasing urbanization reduces precipitation. But this result has to be interpreted with care. Equation (3) is a reduced form of a structural equation from a system of three equations, which is given by (we omit the current temperature and precipitation variables for the other stations to save space)

$$P_{s,i,t} = \gamma_{10} + \gamma_{12}\text{Year}_t + \gamma_{13}\text{Urban}_{s,i,t} + \gamma_{14}T_{s,i,t} + \phi_{11}P_{s-1,i,t} + \phi_{12}\text{Urban}_{s-1,i,t} + \phi_{13}T_{s-1,i,t} + \mu_{1s,i,t}, \quad (8)$$

$$T_{s,i,t} = \gamma_{20} + \gamma_{22}\text{Year}_t + \gamma_{23}\text{Urban}_t + \gamma_{24}P_{s,i,t} + \phi_{21}P_{s-1,i,t} + \phi_{22}\text{Urban}_{s-1,i,t} + \phi_{23}T_{s-1,i,t} + \mu_{2s,i,t}, \quad (9)$$

and

$$\text{Urban}_{s,i,t} = \gamma_{30} + \lambda_{32}\text{Year}_t + \gamma_{33}P_{s,i,t} + \gamma_{34}T_{s,i,t} + \phi_{31}P_{s-1,i,t} + \phi_{32}\text{Urban}_{s-1,i,t} + \phi_{33}T_{s-1,i,t} + \mu_{3s,i,t}; \quad (10)$$

in which the null hypothesis  $\beta_2 = 0$  in Eq. (3) is an indirect test of  $\gamma_{13} = 0$  in Eq. (8). Recovering the value of  $\gamma_{13}$  from the regression coefficients estimated for Eq. (3) requires identifying restrictions. Due to feedback effects of urbanization on temperature ( $\gamma_{23} \neq 0$ ), which

TABLE 2. The value of  $\theta_2$  in Eq. (11). Coefficients are statistically significantly different from zero at \*\*1%, \*5%, and +10% levels. Equation (11) is estimated using ordinary least squares (\$), random effects (#), or the random coefficient model (†).

	Winter	Spring	Summer	Fall
Frac03	-2.66*\$	-20.35†	-2.73†	-23.84†
ED03	-0.01\$	0.02†	1.48E-2†	1.00E-03†
LSI03	-0.02*\$	-2.81E-4†	-0.07*†	-0.02*†
Frac10	-2.44\$	-34.94†	27.19†	-11.84†
ED10	-0.37\$	-1.00**†	-0.04†	0.46*†
LSI10	-1.97+*\$	-29.03*†	5.46†	-11.83*†
Frac20	-3.34\$	-4.72†	-79.04†	-34.56*†
ED20	-2.36+*\$	-2.92†	-1.18†	-10.14*†
LSI20	-2.68+*\$	-2.50†	0.51†	-10.13*†

measures the urban heat island effect, and a contemporaneous relationship between temperature and precipitation ( $\gamma_{14} \neq 0$  and  $\gamma_{24} \neq 0$ ), we cannot identify the system and therefore cannot recover the value of  $\gamma_{13}$ .

Instead, we explore the nature (positive or negative) of the relationship between urbanization and precipitation by estimating the following equation:

$$P_{s,i,t} = \theta_0 + \theta_1\text{Year} + \theta_2\text{Urban}_{s,i,t} + \theta_3T_{s,i,t} + \theta_4\left(\frac{1}{N-1} \sum_{k=1, k \neq i}^N T_{s,k,t}\right) + \theta_5\left(\frac{1}{N-1} \sum_{k=1, k \neq i}^N P_{s,k,t}\right) \quad (11)$$

and use the sign on  $\theta_2$  to proxy the sign of the effect of urbanization on precipitation ( $\gamma_{13}$ ). As indicated in Table 2, the sign of  $\theta_2$  is consistent with the negative value of  $\beta_2$  that is estimated from Eq. (3). This too suggests that urbanization reduces local precipitation.

The seasonal nature of the causal relationship between urbanization and precipitation indicates that the results are not a statistical artifact and suggests several possible mechanisms for an urban precipitation deficit. There is no causal relationship between urbanization and precipitation during the summer. Summer coincides with the rainy season, when the East Asian monsoon has a dominant effect at spatial scales far beyond urban areas. As such, the magnitude of this effect may overwhelm local urban impacts.

During the dry season, cold fronts from northern China bring some rainfall but with a much smaller magnitude and thus local urban effects may be more visible. This may explain why the UHI is most visible in winter (Zhou et al. 2004). The causal relationship indicates that the level of urbanization within the 10- and 20-km buffers influences local synoptic events.

Within buffers, urbanization may reduce precipitation by changing surface properties, such as vegetation cover, roughness, and albedo, energy flows, and/or water flows in ways that reduce water supplies to the local atmosphere. Structures associated with urban areas may change surface hydrology in ways that accelerate runoff via storm water management, which would reduce surface storage and ultimately the water that is available for evaporation. This effect may be exacerbated by a reduction in vegetative cover, which would slow the transfer of water from the soil to the atmosphere via evapotranspiration. This notion is supported by empirical analyses that indicate urbanization reduces the fraction of net radiation that is used for evaporative processes (Carlson and Arthur 2000; Arthur-Hartranft et al. 2003).

Our results also are consistent with previous studies that show a tight coupling between air pollution and precipitation (Cerveny and Balling 1998). The reduction in precipitation may be amplified by increased emissions of air pollutants. A significant increase in aerosol concentrations could increase cloud condensation nuclei and thereby reduce precipitation (Rosenfeld 2000; Crutzen 2004). However, other studies indicate that the net effect of aerosols is to cool the climate system (Kaufman et al. 2002), suggesting that the heat island effect could be partially offset by the cooling caused by aerosols (Chen et al. 2006).

These negative effects on precipitation may be larger than urbanization's other effects, which could boost precipitation by increasing surface roughness and/or convection. Increased convection associated with the urban heat island effect probably does not generate the causal effect of urbanization on precipitation that is estimated from Eq. (3). Because this equation includes temperature, eliminating the urbanization variable from Eq. (3) does not eliminate the effect of urbanization on convection via the urban heat island effect. The potential for conflicting effects implies that the relationship between urbanization and precipitation may vary by location.

The Pearl River Delta has one of the highest rates of urbanization in the world: during the 9-yr period, urban areas increased 300% (Seto et al. 2000). Although these high rates may make the effect easier to detect, the effect of urbanization on precipitation probably is not restricted to the Pearl River Delta of China. Large areas of the United States have been paved or "built up" such that they are now considered "impervious surface areas." This implies that anthropogenic changes in land use could have significant effects on local precipitation throughout the world.

*Acknowledgments.* This research was supported by the U.S. National Science Foundation, CAREER Program, Grant BCS-348986 (Seto).

#### REFERENCES

- Arnfield, A. J., 2003: Two decades of urban climate research: A review of turbulence, exchanges of energy and water, and the urban heat island. *Int. J. Climatol.*, **23**, 1–26.
- Arthur-Hartranft, T., N. Carlson, and K. C. Clarke, 2003: Satellite and ground-based microclimate and hydrological analyses coupled with a regional urban growth model. *Remote Sens. Environ.*, **86**, 385–400.
- Banta, R. M., and Coauthors, 1998: Daytime buildup and nighttime transport of urban ozone in the boundary layer during a stagnation episode. *J. Geophys. Res.*, **103**, 22 519–22 544.
- Bornstein, R., and Q. Lin, 2000: Urban heat islands and summertime convective thunderstorms in Atlanta: Three cases studies. *Atmos. Environ.*, **34**, 507–516.
- Carlson, T. N., and S. T. Arthur, 2000: The impact of land use/land cover changes due to urbanization on surface microclimate and hydrology: A satellite perspective. *Global Planet. Change*, **25**, 49–65.
- Cerveny, R. S., and R. C. Balling, 1998: Weekly cycles of air pollutants, precipitation and tropical cyclones in the coastal NW Atlantic region. *Nature*, **394**, 561–563.
- Chen, L. X., W. L. Li, W. Q. Zhu, X. J. Zhou, Z. J. Zhou, and H. L. Liu, 2006: Seasonal trends of climate change in the Yangtze Delta and its adjacent regions and their formation mechanisms. *Meteor. Atmos. Phys.*, **92**, 11–23.
- Crutzen, P. J., 2004: New directions: The growing urban heat and pollution island effect—Impact on chemistry and climate. *Atmos. Environ.*, **38**, 3539–3540.
- Deosthali, V., 2000: Impact of rapid urban growth on heat and moisture islands in Pune City, India. *Atmos. Environ.*, **34**, 2745–2754.
- Dixon, P. G., and T. L. Mote, 2003: Patterns and causes of Atlanta's urban heat island—initiated precipitation. *J. Appl. Meteor.*, **42**, 1273–1284.
- Granger, C. W. J., 1969: Investigating causal relations by econometric models and cross-spectral methods. *Econometrica*, **37**, 424–438.
- , 1980: Testing for causality: A personal viewpoint. *J. Econ. Dyn. Control*, **2**, 329–352.
- , and L. Huang, 1997: Evaluation of panel data models: Some suggestions from time series. Department of Economics, University of California, San Diego, Rep. 97-10, 29 pp.
- Hsiao, C., 1986: *Analysis of Panel Data*. Cambridge University Press, 246 pp.
- Ji, C. P., W. D. Liu, and C. Y. Xuan, 2006: Impact of urban growth on the heat island in Beijing. *Chin. J. Geophys.*, **49**, 69–77.
- Kanda, M., 2006: Progress in the scale modeling of urban climate: Review. *Theor. Appl. Climatol.*, **84**, 23–34.
- Kaufman, Y. J., D. Tanre, and O. Boucher, 2002: A satellite view of aerosols in the climate system. *Nature*, **419**, 215–223.
- Kaufmann, R. K., and K. C. Seto, 2001: Change detection, accuracy, and bias in a sequential analysis of Landsat imagery: A time series technique. *Agric. Ecosyst. Environ.*, **85**, 95–105.
- , L. Zhou, R. B. Myneni, C. J. Tucker, D. Slayback, N. V. Shabanov, J. Pinzon, 2003: The effect of vegetation on surface temperature: A statistical analysis of NDVI and climate data. *Geophys. Res. Lett.*, **30**, 2147, doi:10.1029/2003GL018251.

- Lehmann, E. L., 1975: *Nonparametrics: Statistical Methods Based on Ranks*. Holden-Day, 457 pp.
- Lo, C. P., D. A. Quattrochi, and J. C. Luvall, 1997: Application of high-resolution thermal infrared remote sensing and GIS to assess the urban heat island effect. *Int. J. Remote Sens.*, **18**, 287–304.
- Lowry, W. P., 1998: Urban effects on precipitation. *Prog. Phys. Geogr.*, **22** (4), 477–520.
- McGarigal, K., and B. J. Marks, 1995: Fragstats: Spatial pattern analysis program for quantifying landscape structure. Tech. Rep. PNW-GTR-351, 122 pp. [Available from Pacific Northwest Research Station, USDA-Forest Service, Portland, OR 97204.]
- Molders, N., and M. A. Olson, 2004: Impact of urban effects on precipitation in high latitudes. *J. Hydrometeor.*, **5**, 409–429.
- Mosedale, T. J., D. B. Stephenson, M. Collins, and T. C. Mills, 2006: Granger causality of coupled climate processes: Ocean feedback on the North Atlantic Oscillation. *J. Climate*, **19**, 1182–1194.
- Mundlak, Y., 1978: On the pooling of time series and cross section data. *Econometrica*, **46**, 69–85.
- Oke, T. R., 1976: City size and the urban heat island. *Atmos. Environ.*, **7**, 769–779.
- Pataki, D. E., D. R. Bowling, and J. R. Ehleringer, 2003: Seasonal cycle of carbon dioxide and its isotopic composition in an urban atmosphere: Anthropogenic and biogenic effects. *J. Geophys. Res.*, **108**, 4735, doi:10.1029/2003JD003865.
- Rosenfeld, D., 2000: Suppression of rain and snow by urban and industrial air pollution. *Science*, **287**, 1793–1796.
- Seto, K. C., 2004: Urban growth in South China: Winners and losers of China's policy reforms. *Petermanns Geogr. Mitt.*, **148** (5), 50–57.
- , and R. K. Kaufmann, 2003: Modeling the drivers of urban land use change in the Pear River Delta, China: Integrating remote sensing with socioeconomic data. *Land Econ.*, **79**, 106–121.
- , and M. Fragkias, 2005: Quantifying spatiotemporal patterns of urban land-use change in four cities of China with time series landscape metrics. *Landscape Ecol.*, **20**, 871–888.
- , R. K. Kaufmann, and C. E. Woodcock, 2000: Landsat reveals China's farmland reserves, but they're vanishing fast. *Nature*, **406**, 121.
- , E. Woodcock, C. Song, X. Huang, J. Lu, and R. K. Kaufmann, 2002: Monitoring land-use change in the Pearl River Delta using Landsat TM. *Int. J. Remote Sens.*, **23**, 1985–2004.
- Shepherd, J. M., 2005: A review of current investigations of urban-induced rainfall and recommendations for the future. *Earth Interactions*, **9**. [Available online at <http://EarthInteractions.org>.]
- , H. Pierce, and A. J. Negri, 2002: Rainfall modification by major urban areas: Observations from spaceborne rain radar on the TRMM satellite. *J. Appl. Meteor.*, **41**, 689–701.
- Souch, C., and S. Grimmond, 2006: Applied climatology: Urban climate. *Prog. Phys. Geogr.*, **30** (2), 270–279.
- Tereshchenko, I. E., and A. E. Filonov, 2001: Air temperature fluctuations in Guadalajara, Mexico, from 1926 to 1994 in relation to urban growth. *Int. J. Climatol.*, **21**, 483–494.
- Thielen, J., W. Wobrock, A. Gadian, P. G. Mestayer, and J.-D. Creutin, 2000: The possible influence of urban surfaces on rainfall development: A sensitivity study in 2D in the mesogammascale. *Atmos. Res.*, **54**, 15–39.
- UNCHS, cited 2002: The state of the world's cities report 2001. United Nations Centre for Human Settlements (Habitat). [Available online at <http://ww2.unhabitat.org/Istanbul+5/statereport.htm>.]
- Voogt, J. A., and T. R. Oke, 2003: Thermal remote sensing of urban climate. *Remote Sens. Environ.*, **86**, 370–384.
- Wang, W., Z. Zeng, and T. R. Karl, 1990: Urban heat islands in China. *Geophys. Res. Lett.*, **17**, 2377–2380.
- Weng, Q., 2002: Land use change analysis in the Zhujiang Delta of China using satellite remote sensing, GIS and stochastic modeling. *J. Environ. Manage.*, **64**, 273–284.
- Yeh, A. G. O., and X. Li, 1997: An integrated remote sensing and GIS approach in the monitoring and evaluation of rapid urban growth for sustainable development in the Pearl River Delta, China. *Int. Plann. Stud.*, **2**, 193–210.
- , and —, 1998: Sustainable land development model for rapid growth areas using GIS. *Int. J. Geogr. Info. Sci.*, **2**, 169–189.
- Zhang, J. Y., W. J. Dong, L. Y. Wu, J. F. Wei, P. Y. Chen, and D. K. Lee, 2005: Impact of land use changes on surface warming in China. *Adv. Atmos. Sci.*, **22** (3), 343–348.
- Zhou, L., R. E. Dickinson, Y. Tian, J. Fang, Q. Li, R. K. Kaufmann, C. J. Tucker, and R. B. Myneni, 2004: Evidence for a significant urbanization effect on climate in China. *Proc. Natl. Acad. Sci. USA*, **101**, 9540–9544.